

Broad temperature range of cubic blue phase existed in simple binary mixture systems containing rodlike Schiff base mesogens with tolane moiety

Chiung-Cheng Huang^{*a}, Yu-Hao Chen^a, Sheng-Yen Chen^a, Yi-Zeng Sun^a,
Zong-Ye Wu^a, Mei-Ching Yu^a, Bo-Hao Chen^b, I-Jui Hsu^{*b}, Lai-Chin
Wu^c and Jey-Jau Lee^c

^aDepartment of Chemical Engineering, Tatung University, Taipei 104, Taiwan E-mail: chchhuang@ttu.edu.tw

^bDepartment of Molecular Science and Engineering, National Taipei University of Technology, Taipei 106, Taiwan
E-mail: ijuihsu@ntut.edu.tw

^cNational Synchrotron Radiation Research Center of Taiwan, Hsinchu 300, Taiwan
Electronic supplementary information (ESI)

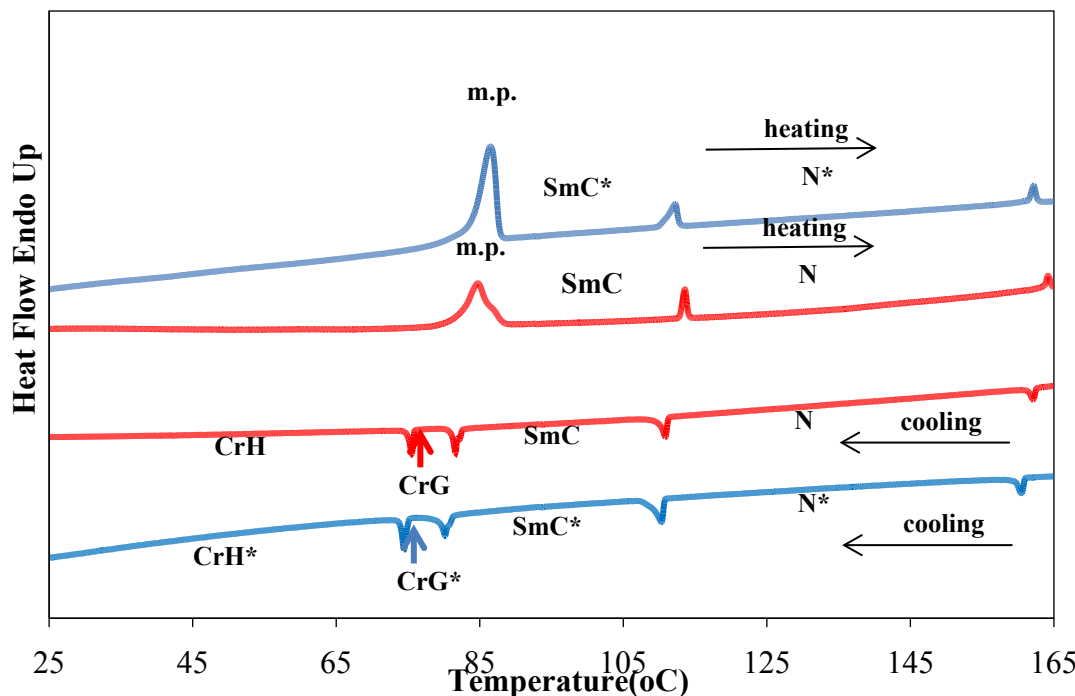


Fig. S1 The DSC measurement of compounds (*S*)-OH-TI (blue line) and OH-TI (red line) on heating and cooling recycle.

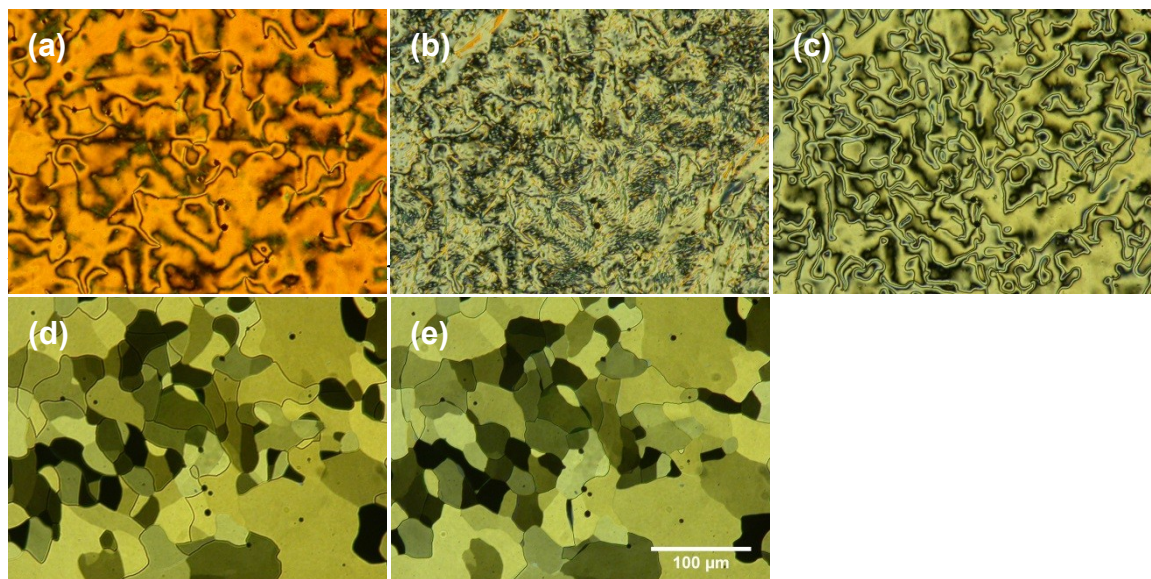


Fig. S2 Microphotographs for compound **OH-TI**

(a) N texture at 149.3°C; (b) N - SmC texture at 110.4°C; (c) SmC texture at 100.0°C;
(d) CrG texture at 79.8°C; (e) CrH texture at 68.0°C.

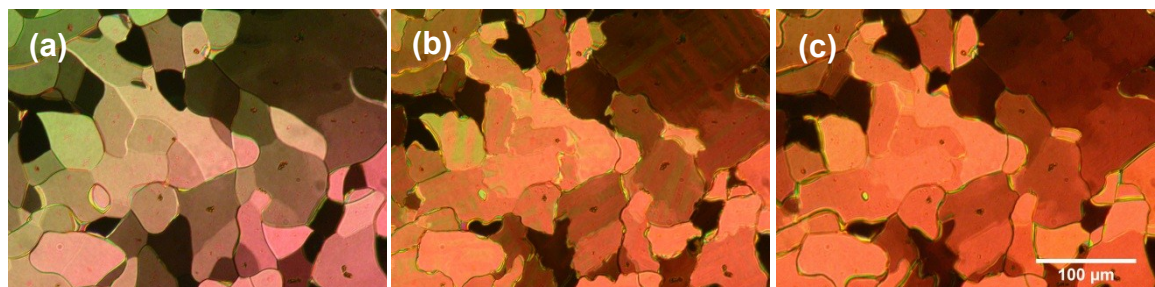


Fig S3. Transition from mosaic texture of the soft crystal G to the soft crystal H of compound **OH-TI₇** observed in the other area. (a) CrG texture at 78.6°C; (b) CrG-CrH texture at 75.8°C; (c) CrH texture at 70.0°C.

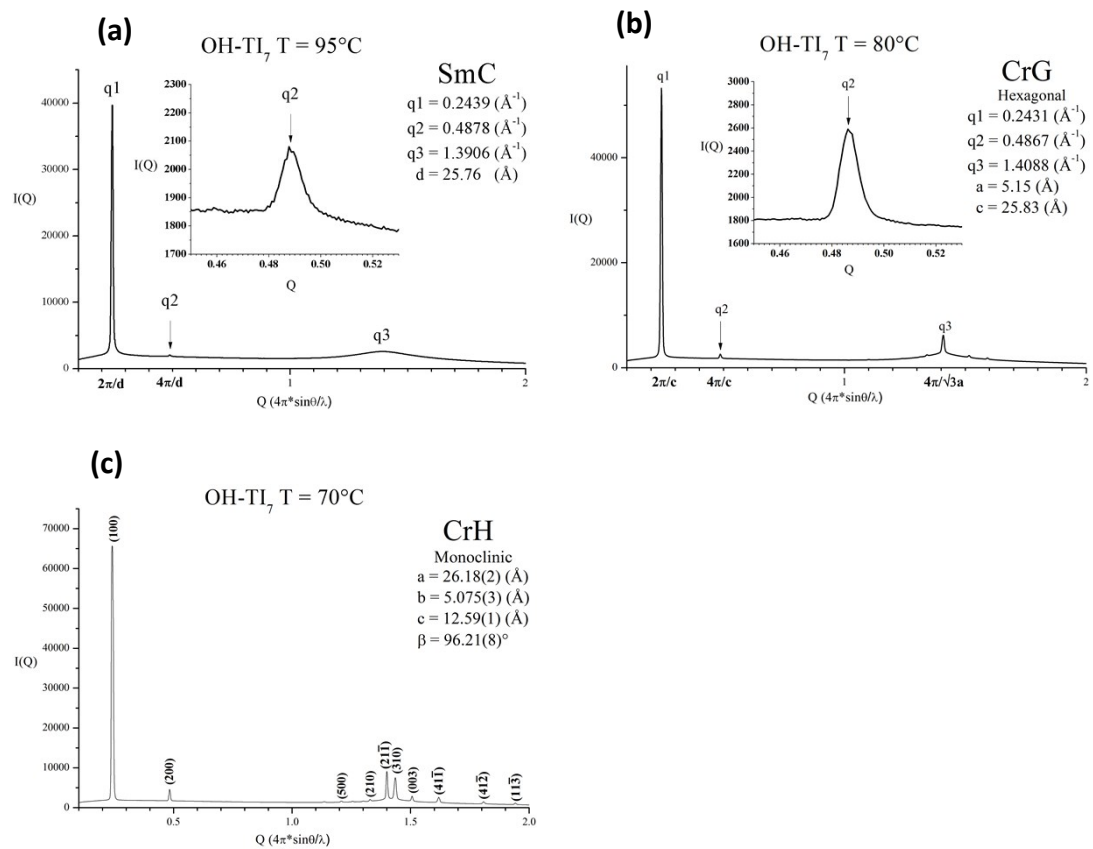


Fig. S4 The variable-temperature XRD measurements of compound OH-TI₇.

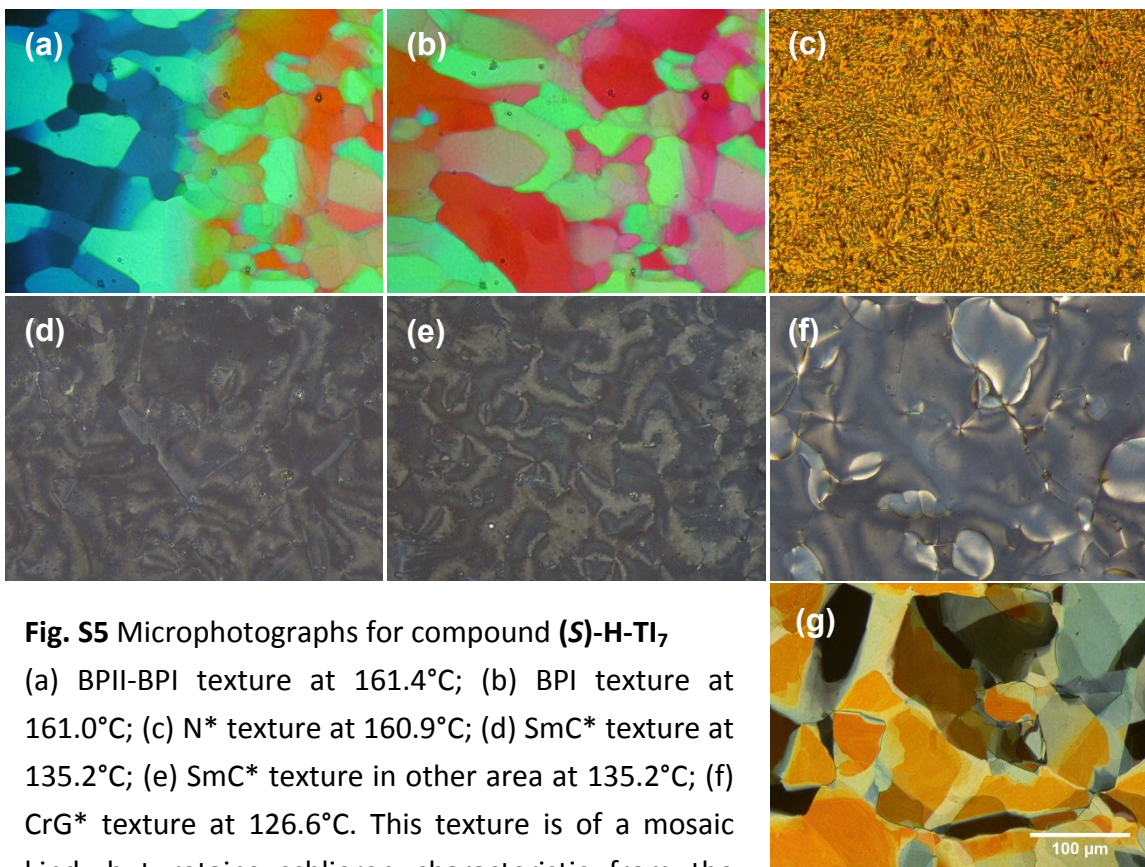


Fig. S5 Microphotographs for compound **(S)-H-TI**,

(a) BPII-BPI texture at 161.4°C; (b) BPI texture at 161.0°C; (c) N* texture at 160.9°C; (d) SmC* texture at 135.2°C; (e) SmC* texture in other area at 135.2°C; (f) CrG* texture at 126.6°C. This texture is of a mosaic kind, but retains schlieren characteristic from the smectic C phase ; (g) CrH* texture at 99.8°C.

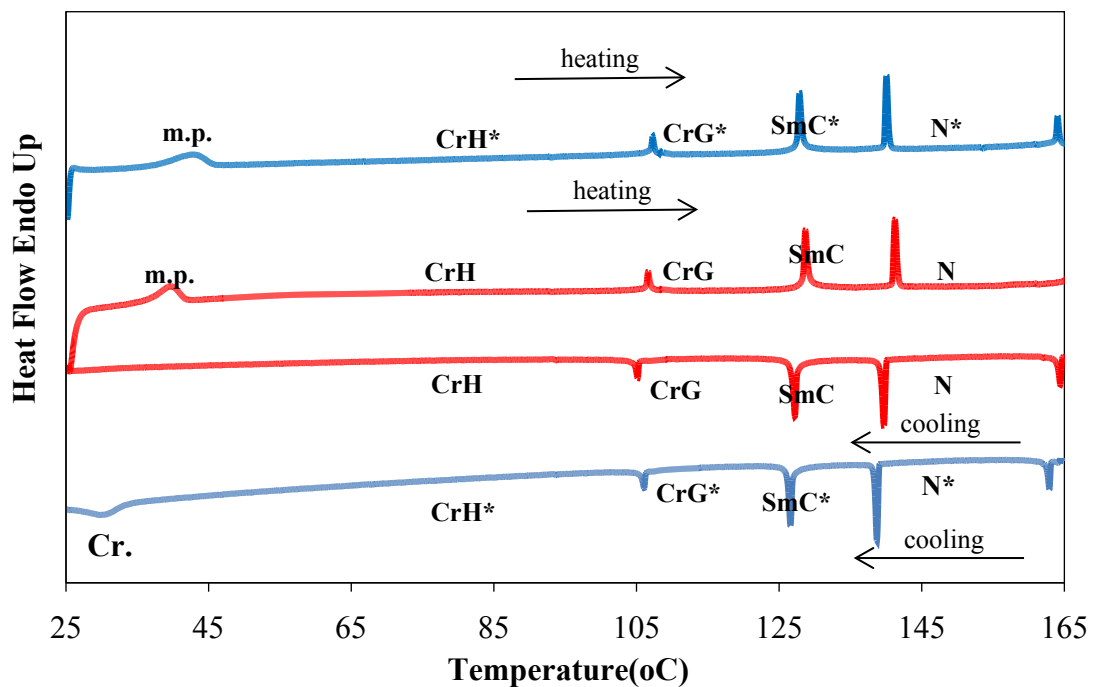


Fig. S6 The DSC measurement of compounds **(S)-H-TI** (blue line) and **H-TI** (red line) on heating and cooling recycle.

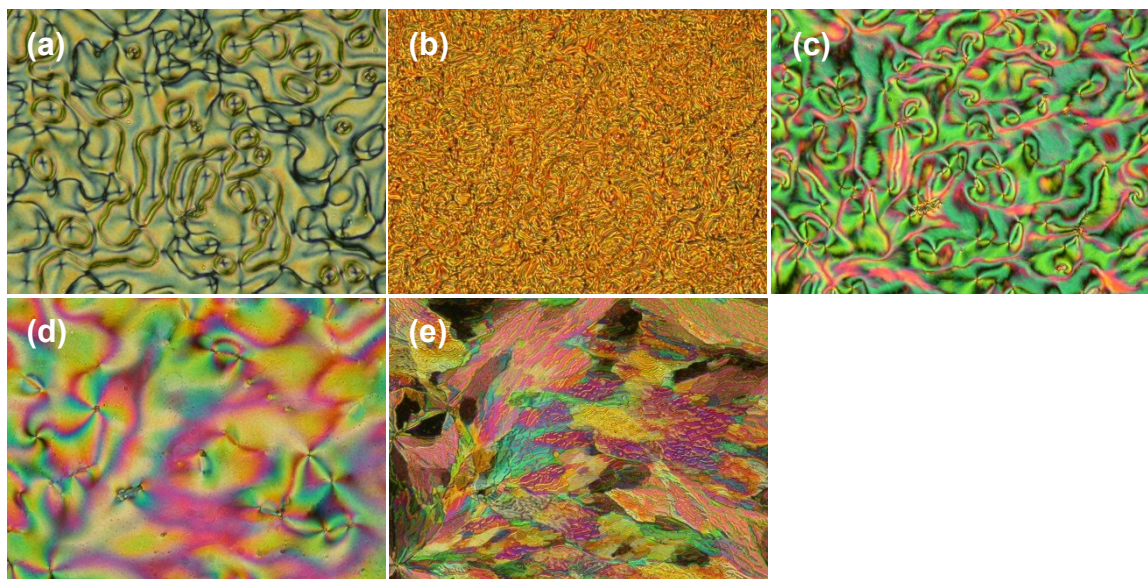


Fig. S7 Microphotographs for compound H-TI

(a) N texture at 149.8°C; (b) N-SmC texture at 139.8°C; (c) SmC texture at 136.1°C;
(c) CrG texture at 121.9°C; (d) CrH texture at 101.8°C.

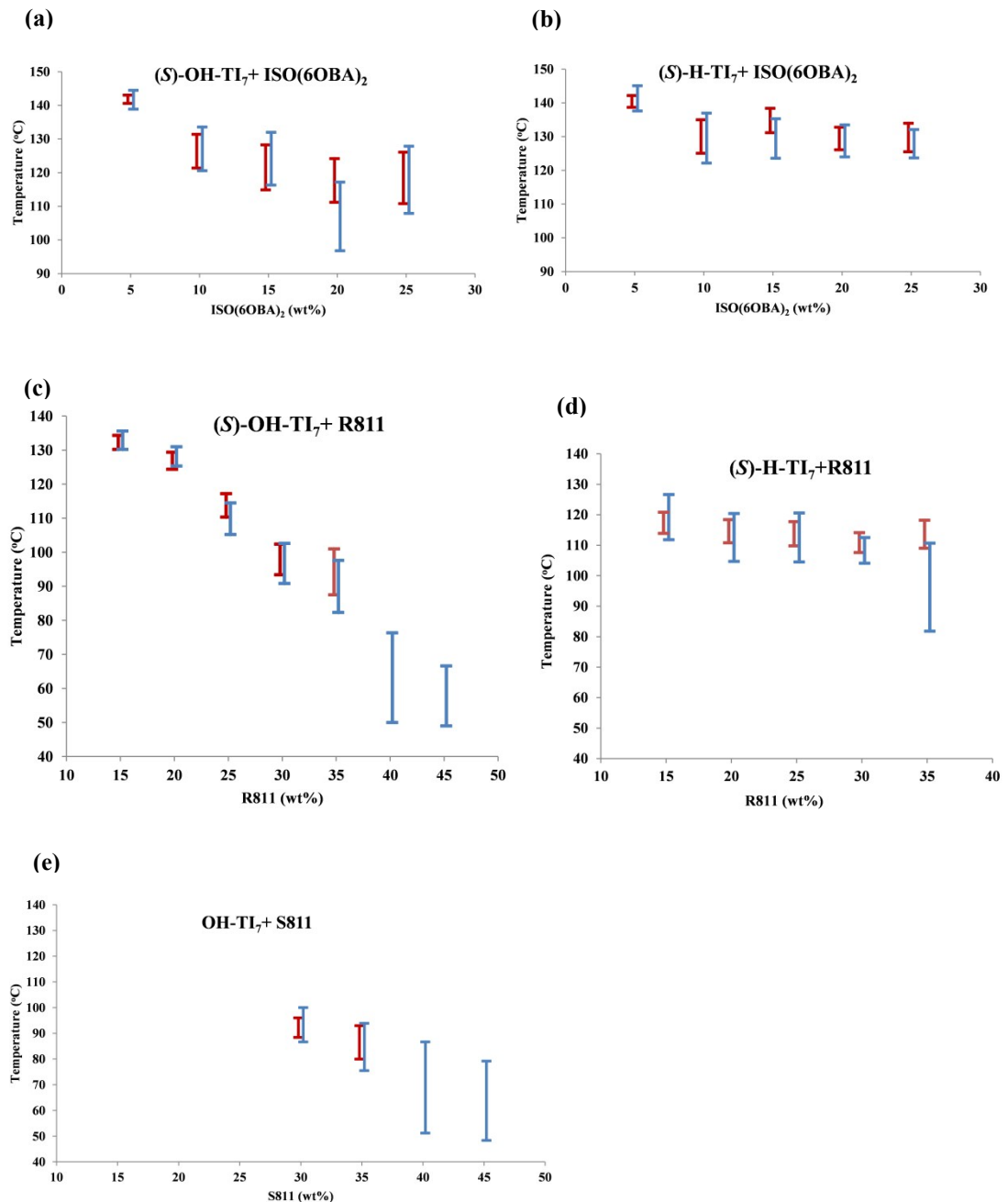


Fig. S8 The comparison of BP temperature range for the different blending mixture systems in heating (red line) and cooling processes (blue line).

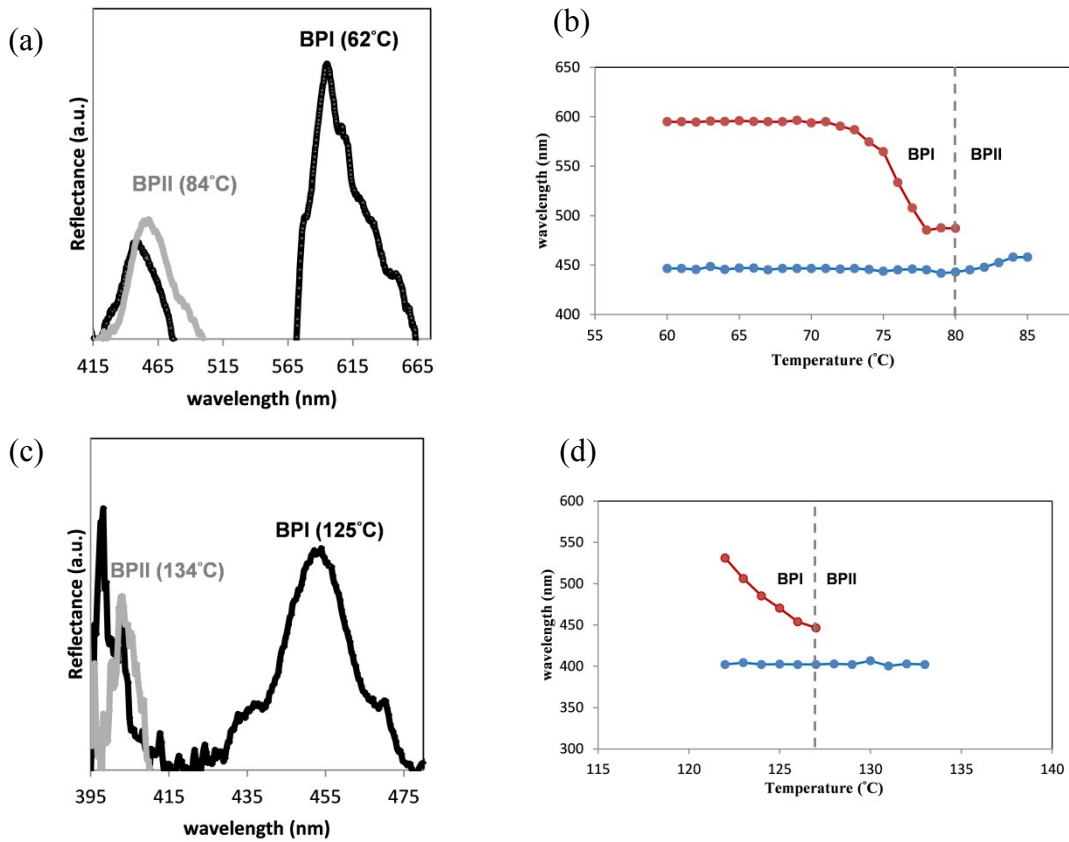


Fig. S9 Typical reflectance profiles of the higher-temperature phase (gray line) and the lower-temperature phase (black line) for the blending system mixture (a) **OH-TI₇** + 40% **S811** and (c) **(S)-OH-TI₇** + 10% **IOS(6OBA)₂**. Temperature dependence of the Bragg reflection wavelength for the blending mixture consisting of **OH-TI₇** + 40% **S811** (b) and **(S)-OH-TI₇** + 10% **IOS(6OBA)₂** (d) during cooling process with a rate of 0.5 °C min⁻¹.

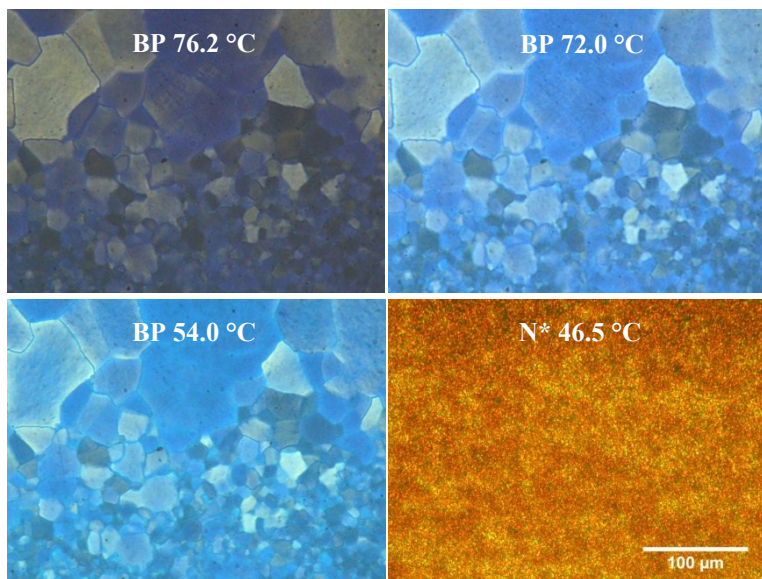


Fig. S10 Microphotographs for compound **(S)-OH-TI** blended with 40.0 wt% **R811**.

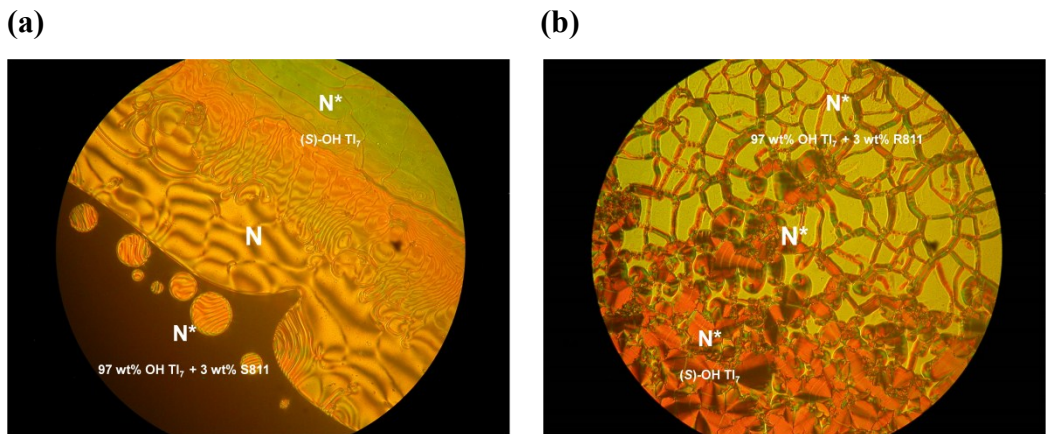


Fig. S11 Contact test of Schiff base **(S)-OH-TI₇** and the mixture of racemic Schiff base **OH-TI₇** doped with 4 wt% **S811** (a) and **R811** (b).

Measurements of helical pitch and helical twisting power of two chiral Schiff base mesogens and binary mixture system composed of 60 wt% racemic Schiff base and 40 wt% S811 by Cano's Wedge method.

The helical pitch (p) was evaluated by measuring the distance (a) between Cano lines as follows: $p = 2a \tan\theta$, where θ is the angle of the wedge of the cell.

In this experiment, the cell's $\tan\theta$ is 0.0196, the concentration of the chiral dopant c is 4%.

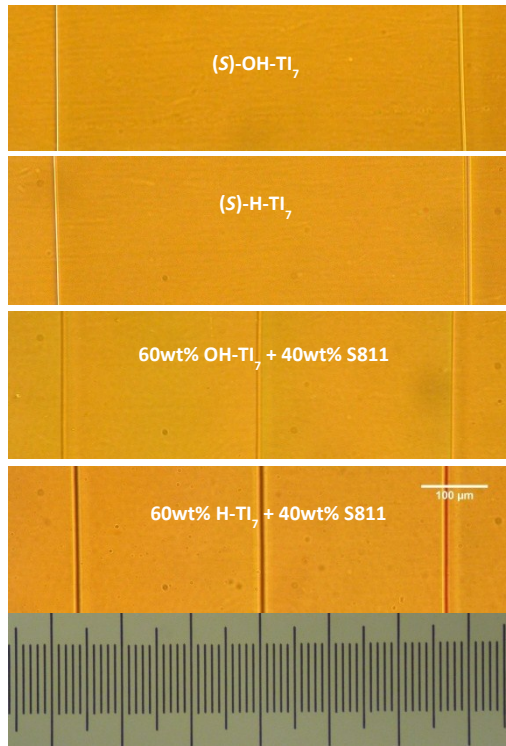


Fig. S12 Cano's Wedge method to measure the helical pitch of two chiral Schiff base mesogens and binary mixture system composed of 60 wt% racemic Schiff base and 40 wt% **S811**.

The DSC diagram, POM texture and XRD variable-temperature XRD of Schiff base mesogen OH-TI₇₇.

The DSC (Fig. S13) and POM pictures (Fig. S14) have indicated that Schiff base compound **OH-TI₇₇**, on cooling from its isotropic phase, displayed nematic Schlieren texture (N phase, Fig. S14a), straited texture below N-SmC transition (Fig. S14b), Schlieren texture with narrow dark four brushes (SmC phase, Fig. S14c), Schlieren texture with broader dark four-brushes (SmF phase, Fig. S14d), mosaic terrace-like relief with larger domains (the soft crystal CrG phase, Fig. S14e), mosaic texture with small platelet area that are cross-hatched by grainings (the soft crystal CrH phase, Fig. S14f) and two crystal phase (Fig. S14g and Fig. S14h).

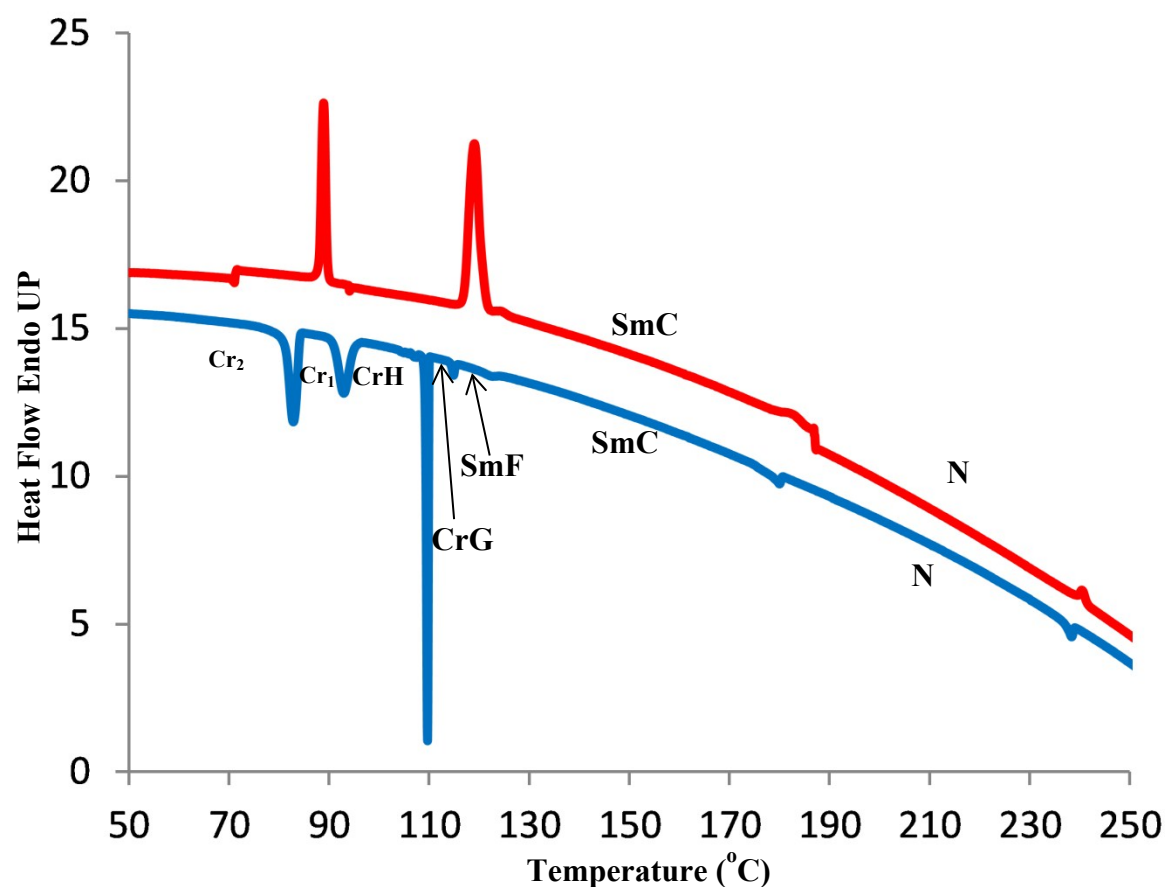


Fig. S13 The DSC measurement of compounds **OH-TI₇₇** on heating (red line) and cooling recycle (blue line).

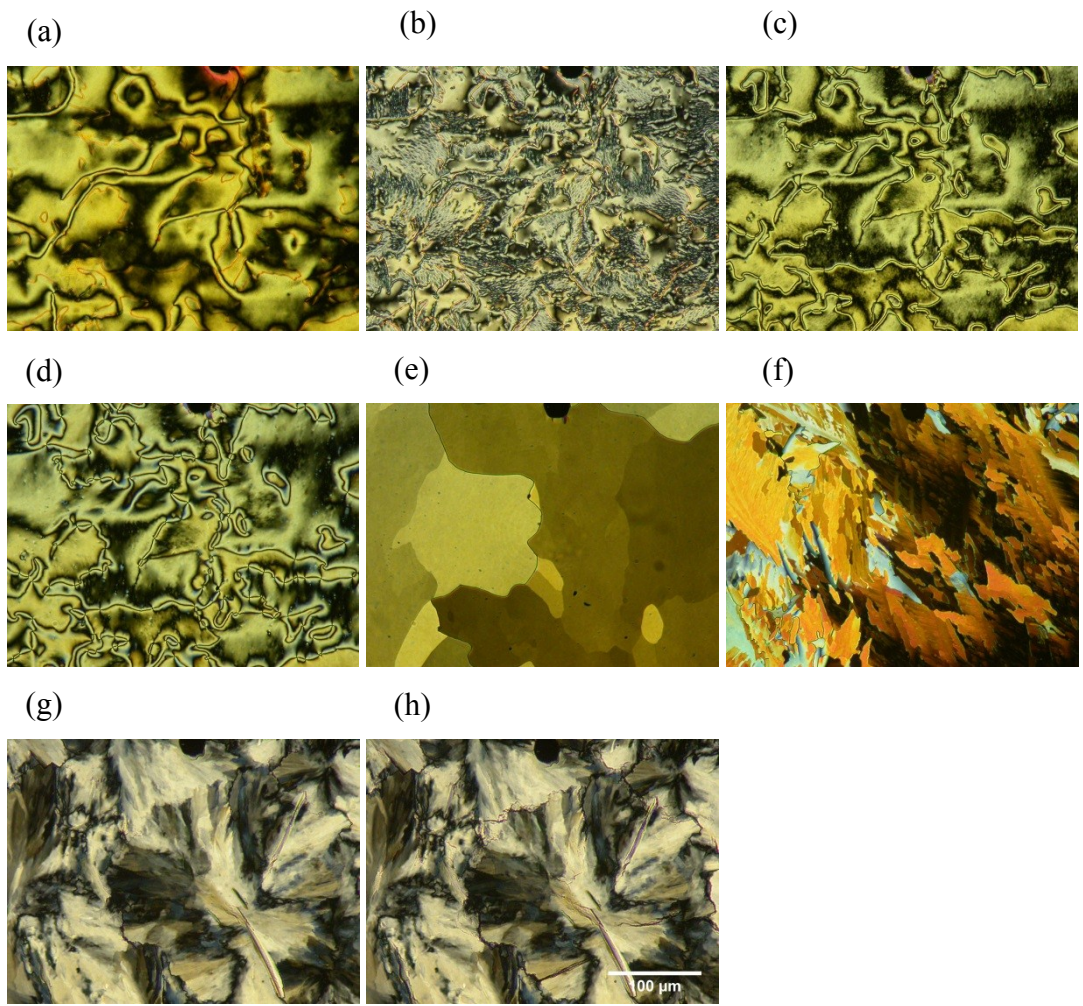


Fig. S14 Microphotographs of compound **OH-TI₇₇** observed under the POM: (a) N texture at 210.0°C; (b) N - SmC transition texture at 181.6°C; (c) SmC texture at 130.0°C; (d) SmF texture at 120.0°C; (e) CrG texture at 112.0°C; (f) CrH texture at 100.0°C; (g) Cr₁ texture at 87.8°C; (h) Cr₂ texture at 74.2°C.

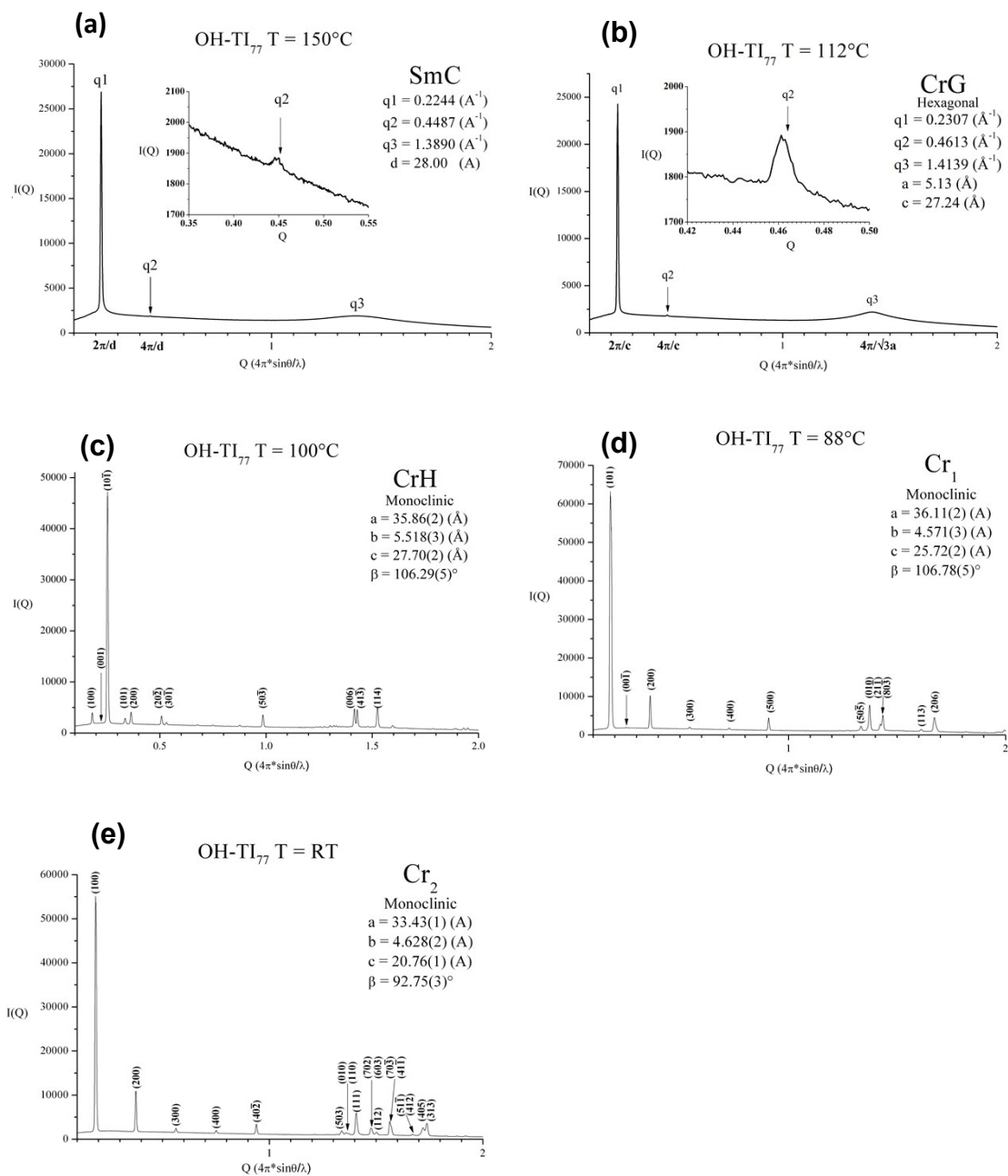
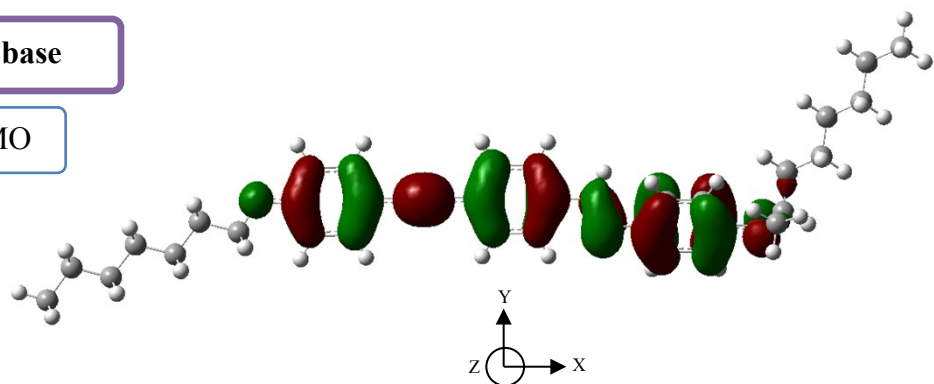


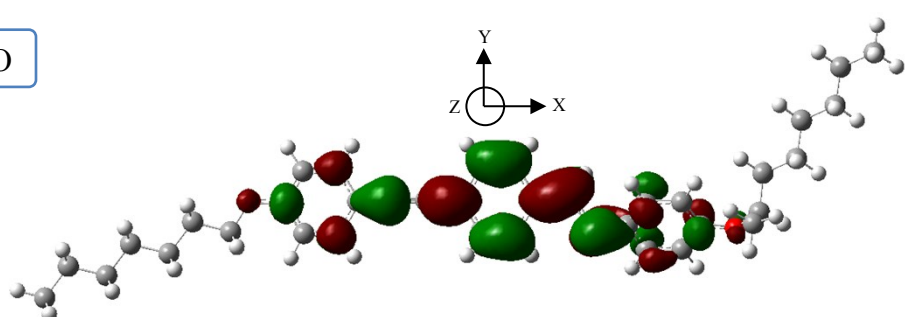
Fig. S15 The variable-temperature XRD measurements of compound OH-TI₇₇.

Schiff base

HOMO

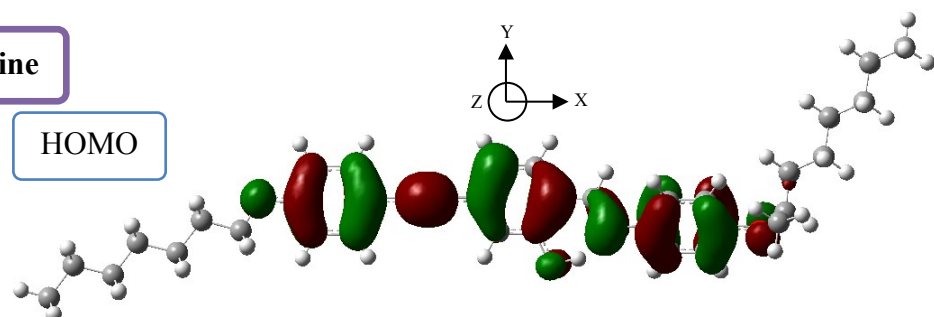


LUMO

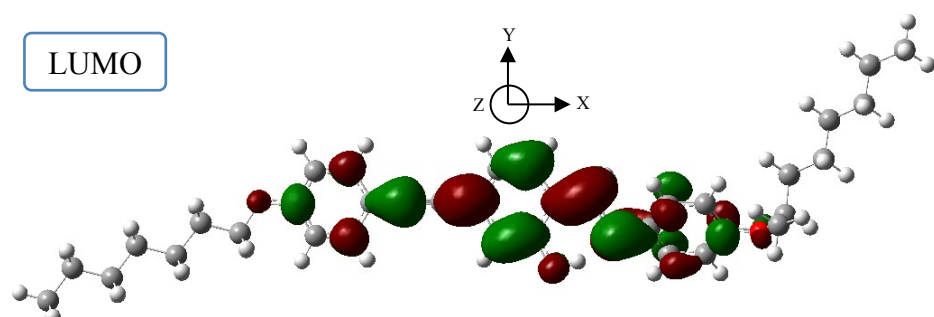


Salicylaldimine

HOMO

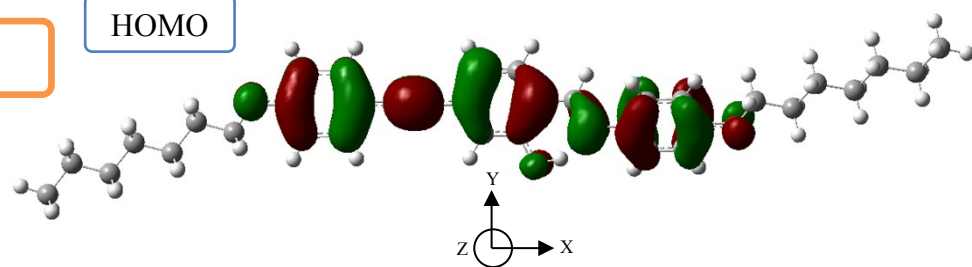


LUMO



OH-TI₇₇

HOMO



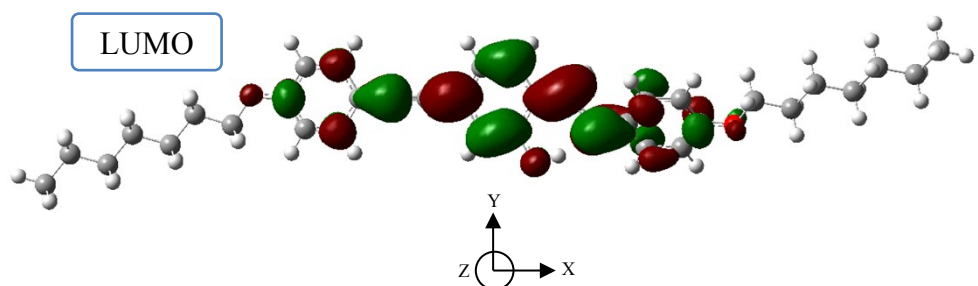


Fig. S16. HOMO and LUMO of **Schiff base** compound (a), **Salicylaldimine** compound (b) and compound **OH-Tl₇₇** (c). The simulation exchange functional and basis set are CAM-B3LYP and 6-311G(d, p), respectively. The isosurface is drawn at value of 0.02.

Table S1. A comparison table with different basis sets and exchange functionals on the calculated dipole moment in **Schiff base** compound, **Salicylaldimine** compound and compound **OH-TI₇₇**.

Exchange functional	Basis set	Dipole Moment (Debye)		
		Schiff base	Salicylaldimine	OH-TI ₇₇
CAM-B3LYP	6-311G(d,p)	1.8072	2.2053	1.9450
	def2-tzvp	1.9057	2.1953	1.9520
	6-31G(d)	1.8032	2.1847	1.9789
	6-31+G(d)	1.9425	2.3394	2.1277
ω B97X	6-311G(d,p)	1.6789	2.3066	1.9574
	6-31G(d)	1.6739	2.0637	2.0152
	6-31+G(d)	2.1211	2.1983	2.0575

Table S2. DFT calculated HOMO, LUMO, energy gap, dipole moment components, μ_x , μ_y , μ_z and modulus (μ) for **Schiff base** compound, **Salicylaldimine** compound and compound **OH-TI₇₇**.

Exchange functional and Basis set	Compound	Energy (eV)			Dipole moment (μ in Debye)			
		HOMO	LUMO	ΔE (eV)	μ_x	μ_y	μ_z	μ_{total}
CAM-B3LYP 6-311G(d,p)	Schiff base	-6.697	-0.764	5.933	-1.058	-0.850	1.194	1.807
	Salicylaldimine	-6.736	-0.842	5.894	0.543	1.772	1.195	2.205
	OH-TI₇₇	-6.766	-0.860	5.906	0.296	1.775	0.738	1.945
ω B97X 6-311G(d,p)	Schiff base	-7.641	0.116	7.757	-0.937	1.391	0.084	1.679
	Salicylaldimine	-7.689	0.034	7.723	0.478	1.671	1.518	2.307
	OH-TI₇₇	-7.701	0.014	7.715	0.286	1.817	0.669	1.957

Table S3. DFT calculated principal polarizability components (α_{XX} , α_{YY} , α_{ZZ}), isotropic component $\alpha^{\text{iso}} = (\alpha_{XX} + \alpha_{YY} + \alpha_{ZZ})/3$, polarizability anisotropy $\Delta\alpha = [\alpha_{XX} - (\alpha_{YY} + \alpha_{ZZ})/2]$ and asymmetry parameter $\eta_\alpha = [(\alpha_{YY} - \alpha_{ZZ})/(\alpha_{XX} - \alpha^{\text{iso}})]$, relative to the molecular polarizability tensor α .

Exchange functional and Basis set	Compound	α_{XX}	α_{YY}	α_{ZZ}	α^{iso}	$\Delta\alpha$	η_α
CAM-B3LYP 6-311G(d,p)	Schiff base	874.25	374.57	256.32	501.71	558.81	0.31742
	Salicylaldimine	892.29	380.81	256.42	509.84	573.68	0.32525
	OH-TI₇₇	897.57	353.14	246.43	499.05	597.79	0.26777
ω B97X 6-311G(d,p)	Schiff base	818.70	373.20	261.67	484.53	501.27	0.33375
	Salicylaldimine	837.45	376.35	264.11	492.64	517.22	0.32551
	OH-TI₇₇	846.19	351.98	249.84	482.67	545.28	0.28098

References:

1. D. Demus, S. Diele, M. Klapperstück, V. Link a and H. Zaschke, *Mol. Cryst. Liq. Cryst.*, 1971, **15**, 161-174.
2. G. W. Gray and J. W. Goodby, *Smectic Liquid Crystals: Texture and structure*, Leonard Hill, Philadelphia, 1984.
3. I. Dierking, *Textures of Liquid Crystals*, Wiley-VCH, Weinheim, 2003.